2009

Basal Autophagy Induction Without AMP-Activated Protein Kinase Under Low Glucose Conditions

Tyisha Williams
Trinity University, twilliam@trinity.edu

L. J. Forsberg

B. Viollet

J. E. Brenman

Repository Citation

Williams T., Forsberg LJ., Viollet B., & Brenman J (2009). Basal autophagy induction without AMP-activated protein kinase under glucose conditions. *Autophagy, 5*(8), 1-11. doi:10.4161/auto.5.8.10090

Research Paper

Basal autophagy induction without AMP-activated protein kinase under low glucose conditions.

Tyisha Williams[1], Lawrence J. Forsberg[1], Benoit Viollet[2, 3], and Jay E. Brenman[1,4]

[1]The Neuroscience Center UNC Chapel Hill School of Medicine; [2]INSERM U567 Paris, France; [3]Institut Cochin, Université Paris Descartes, CNRS (UMR 8104), Paris, France [4]Cell and Developmental Biology Dept. UNC-CH School of Medicine

Key Words: AMPK, autophagy, apoptosis, p53, PTEN, LC3, ATP, AICAR

Acknowledgements

The authors would like to thank Dr. F. Wang for generously providing the venus-LC3 plasmid. We thank R. Peterson for help with confocal, M. Deshmukh and R. Dumitru for help with the ATP assay. T. Williams would like to thank F. Polleux for his invaluable help. This work was supported by National Institutes of Health (NIH) grants MH073155S (to T.Williams) and MH073155 (to J. Brenman) and NINDS Institutional Center Grant P30- NS45892-01 for Neuroscience Confocal Core and by the European Union FP6 program (EXGENESIS Integrated Project LSHM-CT- 2004-005272 to B. Viollet).

Abbreviations: AMPK, AMP-activated protein kinase; AICAR, 5-aminoimidazole-4-carboxamide ribonucleoside; MEFs, mouse embryonic fibroblasts; 3-MA, 3-

methyladenine; LC3, microtubule-associated protein light chain 3; PI, Propidium Idodide; PARP, poly ADP ribose polymerase; mTOR, mammalian target of rapamycin; TSC1/2, Tuberous Sclerosis Complex 1/2

Correspondence to: J. Brenman, UNC-CH School of Medicine, Chapel Hill, NC 27599-7250 USA email: Brenman@med.unc.edu

When ATP levels in a cell decrease, various homeostatic intracellular mechanisms initiate attempts to restore ATP levels. As a prominent energy sensor, AMP-activated protein kinase (AMPK) represents one molecular gauge that links energy levels to regulation of anabolic and catabolic processes to restore energy balance. Although pharmacological studies have suggested that an AMPK activator, AICAR (5-aminoimidazole-4-carboxamide ribonucleoside) may link AMPK activation to autophagy, a process that can provide short-term energy within the cell, AICAR can have AMPK-independent effects. Therefore, using a genetic-based approach we investigated the role of AMPK in cellular energy balance. We demonstrate that genetically altered cells, mouse embryonic fibroblasts (MEFs), lacking functional AMPK display altered energy balance under basal conditions and die prematurely under low glucose-serum starvation challenge. These AMPK mutant cells appear to be abnormally reliant on autophagy under low glucose basal conditions, and therefore cannot rely further on autophagy like wildtype cells during further energetic stress and instead undergo apoptosis. This data suggests that AMPK helps regulate basal energy levels under low glucose. Further, AMPK mutant cells show increased basal phosphorylation of p53 at serine 15, a residue

phosphorylated under glucose deprivation. We propose that cells lacking AMPK function have altered p53 activity that may help sensitize these cells to apoptosis under energetic stress.

Running Title: AMPK promotes low glucose serum deprivation survival

Introduction

Autophagy and apoptosis represent two mechanisms that can ultimately lead to cellular self-eradication. Although apoptosis exclusively eliminates cells, autophagy itself can have either a beneficial or detrimental cellular effect depending on the cellular context. It has been suggested that the net outcome of autophagy depends on multiple other events and processes.[1-7] Although evidence in mammals suggests some molecular coupling between autophagy and apoptosis, the exact molecular connection remains unclear.

Organelles and other cellular constituents including lipids, RNA, and proteins can undergo catabolism via macroautophagy, subsequently referred to herein as "autophagy". Autophagy involves the sequestration of bulk cytoplasmic regions into double-membrane vacuoles that fuse their contents with late endosomal and lysosmal compartments for degradation.[4, 6, 8-13] In addition, there are two other specialized forms of autophagy including chaperone-mediated autophagy (CMA) and microautophagy. CMA involves the selective targeting of proteins containing a KFERQ-like peptide motif to lysosomes for degradation.[6, 8, 13-16] Microautophagy involves the pinocytosis of small quantities of cytosol directly by lysosomes.[6, 13, 17]

If a cell under energetic stress cannot restore energy balance it will eventually die. Cell death can be divided into two main mechanisms: apoptosis or necrosis. Apoptosis is a well-characterized programmed cell death event. The hallmarks of apoptosis include caspase activation, cellular shrinkage, pyknosis, and karyorrhexis. Recent evidence suggests a third type of cell death, autophagic cell death (ACD).[3-6, 18, 19] However, whether apoptosis and ACD are indeed uncoupled events or if autophagic failure leads to apoptosis remain unclear.

AMP-activated protein kinase (AMPK) is a serine-theronine kinase involved in sensing energy status in the cell and regulating metabolism. The heterotrimeric protein complex contains a catalytic subunit α and two regulatory subunits, β and γ respectively.[20-24] Cellular stressors including energetic stress, which lowers ATP levels, lead to activation of AMPK activity. In response, activated AMPK then turns on ATP-generating pathways while inhibiting ATP-consuming pathways in order to increase ATP to AMP ratios.[20-24] AMPK is highly conserved with orthologues expressed in plants, yeast, *Drosophila*, *Caenorhabditis* (*C.*) *elegans*, vertebrates and mammals.[21, 23, 25, 26] The first mutations in an AMPK complex gene were identified as mutations in Snf1 (sucrose non-fermenting) protein kinase, the *Saccharomyces cerevisiae* orthologue of AMPKα.[21, 25-28] In yeast, SNF1 has a role in fully inducing autophagy.[29] However, mammalian studies demonstrate conflicting roles for AMPK in autophagy. There have been several studies indicating that AMPK is an inducer of autophagy,[30-32] while there is evidence in hepatocytes that AMPK is an inhibitor of autophagy.[33, 34] In addition, many studies of AMPK and autophagy rely strictly on pharmacological agents, which may have off-target

effects to activate or inhibit AMPK. Indeed, numerous studies demonstrating AICAR dependent but AMPK independent phenotypes exist.[35-39]

In order to investigate the role of AMPK in autophagy and apoptosis without the use of pharmacological activators or inhibitors of AMPK, we took a genetic-based approach. We derived mouse embryonic fibroblasts (MEFs) lacking AMPK activity from genetically engineered mice to study them within an energy deprivation paradigm. Our results indicate that constitutive genetic loss of AMPK function in MEFs under low glucose lead to an increased basal rate of autophagy under serum-rich conditions. Further, due to elevated autophagy basally, genetically null AMPK cells are less equipped to survive stress exerted by further nutrient deprivation and undergo apoptosis.

Results

20 hours serum deprivation leads to apoptotic cell death in AMPK$\alpha^{-/-}$ (null) MEFs. Typical immortalized MEF cells are able to survive serum-free conditions for a brief period of time typically at least 24 hours. Serum deprivation ("starvation") can be used as a paradigm that more subtly mimics nutrient deprivation and is often followed with serum re-introduction to examine growth factor mediated signaling events. However, in this study with low glucose we observed that serum deprivation itself quickly lead to cell death for cells simultaneously lacking both catalytic AMPK subunits, AMPKα1 and AMPKα2 (hereafter referred to as AMPK$^{-/-}$).

AMPK $^{+/+}$ (wildtype) and AMPK$^{-/-}$ MEFs were subjected to a 20-hour period of serum starvation, after which, we observed 30-40% of the AMPK$^{-/-}$ MEFs completely detached and floating in culture media while wildtype MEFs were attached and appeared healthy. To investigate whether the observed phenotype was an apoptotic or necrotic

event we measured indicators to distinguish the two (the Annexin-V FITC /Propidium Idodide (PI) Assay) on samples from both $AMPK^{+/+}$ and $AMPK^{-/-}$ MEFs under serum-rich and serum deprivation conditions. Results from the Annexin-V FITC/ PI Assay indicate that the cell death only observed in the $AMPK^{-/-}$ MEFs under low glucose-serum deprivation and is an apoptotic event (Figure 1A-D). Although, there was a large population of PI/Annexin-V FITC double positive cells indicating death, there was also a large population of single positive Annexin-V FITC positive cells, a marker exclusive for early apoptosis. High glucose-serum-rich or serum deprived conditions for both cell types as well as low glucose-serum starved $AMPK^{+/+}$ MEFs showed no significant amount of cell death and more than 90% of the cells remained viable at 20 hours following serum removal (Figure 1A-C). Therefore our study focuses on low glucose effects on cell survival unless otherwise stated.

Total AMPKα1/α2 protein levels detected with two independent AMPK antibodies demonstrated significant reduction in $AMPK^{-/-}$ MEFs as expected (Figure 1E). In addition, phosphorylated Acetyl-CoA Carboxylase (ACC) at Serine 79, a target site for AMPK activity, was also diminished (Figure 1E). However, it was not eliminated as other kinases, including PKA, have also been demonstrated to phosphorylate ACC.

To further confirm the cell death observed in $AMPK^{-/-}$ MEFs corresponded to an apoptotic event, we performed western blot analyses on these samples using well-established apoptotic markers, activated PARP and cleaved caspase 3. As expected for surviving cells, $AMPK^{+/+}$ and $AMPK^{-/-}$ MEFs under serum-rich conditions did not display significant cleavage of caspase 3 or PARP (poly ADP ribose polymerase) (Figure 1D). However, after 20 hours of serum deprivation a significant increase in caspase 3

and PARP cleavage was observed in AMPK$^{-/-}$ MEFs, indicating apoptosis within this sample of cells but not in its counterpart AMPK$^{+/+}$ wildtype MEFs.

Increased LC3-II in AMPK$^{-/-}$ MEFs under serum-rich conditions compared to AMPK$^{+/+}$ cells. Under conditions of stress, including reduced energy and serum deprivation, cells can maintain viability by recycling cytoplasmic components to generate energy *via* autophagy. Autophagy can act in a pro-survival manner and assist in evading cell death during stressful conditions, which could otherwise lead to death. Since the apoptotic phenotype we observed in the AMPK$^{-/-}$ MEFs was induced under low glucose-serum deprivation we set out to investigate whether there was an impediment in the autophagic pathway in AMPK$^{-/-}$ cells thereby explaining why these cells die during serum deprivation stress. We first exogenously expressed a Venus-LC3 plasmid in our AMPK$^{+/+}$ and AMPK$^{-/-}$ MEFs cultured in high and low glucose media. The modification status of LC3 is a commonly used marker of autophagy. LC3 is quickly processed into cytosolic LC3-I after it is translated. However, upon induction of autophagy LC3-I becomes lipid conjugated with phosphatidylethanolamine (PE) into LC3-II that can then target to membranes of autophagosomes. Although LC3-I appears diffuse throughout the cell, LC3-II appears punctate and associated with vesicular appearing structures. Fusion of LC3 with a fluorescent tag (e.g. Venus or GFP) can be used as a reporter of relative autophagic activity if combined with other assays. Under low glucose-serum-rich conditions, transfected AMPK$^{-/-}$ MEFs expressing Venus-LC3 displayed predominantly punctate localization of the fluorescent signal (Figure 2F), while wildtype MEFs cultured in either high or low glucose, as well as AMPK$^{-/-}$ cells cultured in high glucose media, displayed diffuse cytosolic localization as expected (Figure 2A, K). As a positive control

we added the natural product, rapamycin, an inducer of autophagy. Rapamycin inhibits the activity of mTOR (mammalian target of rapamycin) thereby inducing autophagy. Both rapamycin and serum deprivation were able to induce autophagy in both cell types indicated by the punctate phenotype (Figure 2B. 2D, 2G, 2I, 2L, 2N). We also observed that $AMPK^{-/-}$ MEFs displayed similar venus-LC3 phenotype as $AMPK^{+/+}$ MEFs under all conditions when cultured in high glucose paradigm (Figure 2K-O). These results suggest that $AMPK^{-/-}$ MEFs appear to have an increased basal rate of autophagy induction during the low glucose-serum rich state. High and low glucose conditions resulted in similar venus-LC3 phenotypes for $AMPK^{+/+}$cells and therefore Figure 2A-E is representative of both conditions.

We further wanted to investigate whether or not autophagy is actually functional in these AMPK-lacking cells. Although autophagosomes are being formed it is important to know whether these autophagosomes are capable of completing autophagy and thereby provide energy to the cell. Therefore we used two lysosomal protease inhibitors, E64d and pepstatin A, which allow the formation of autolysosomes but partially prevent the functional completion of autophagy. Increased amounts in the number of LC3-GFP puncta were observed in venus-LC3 transfected $AMPK^{-/-}$ and wildtype cells when treated with E64d and pepstatin A in conjunction with rapamycin or serum deprived condition compared to rapamycin or serum deprivation only (Figure 2B-E, G-J, L-O). Additionally, whole cell lysates treated with and without 10µg/ml of E64d and pepstatin A in low-glucose DMEM media with serum were harvested and used for western blot analysis of endogenous LC3 in $AMPK^{+/+}$ and $AMPK^{-/-}$ MEFs. LC3-II greatly increased in the presence of lysosomal protease inhibitors for both cell types as expected, as LC3-II

itself is degraded by autophagy. However, greater LC3-II was found in AMPK$^{-/-}$ cells with serum, particularly when comparing the ratio of LC3-II to LC3-I (Figure 3A). These Western blot results confirmed that an increased basal rate of autophagy under nutrient rich condition occurs in AMPK$^{-/-}$ MEFs with a 3-fold increase in LC3-II formation in the presence of lysosomal inhibitors (E64d and pepstatin A) compared to conditions without lysosomal inhibitors suggesting at least functional autophagy induction. We also investigated LC3-II formation in cells cultured for 20 hours under serum starvation. Under serum starvation conditions, LC3-II/LC3-I ratios markedly increased in AMPK$^{+/+}$ cells with or without lysosomal protease inhibitors (Figure 3B) compared to lysates from cells with serum (Figure 3A). Both AMPK$^{+/+}$ and AMPK$^{-/-}$ MEFs show increased LC3-II formation in the presence of lysosomal inhibitors as expected for functional autophagy (Figure 3B).

However it is essential, if monitoring autophagy via LC3-II accumulation, that a time course of the autophagic flux be conducted [9, 11]. Therefore we monitored autophagic flux by harvesting serum-deprived cells treated with lysosmal inhibitors at 0, 2, 6, 12, and 20 hours after serum deprivation (Figure 4). As expected, we did not observe LC3-II in AMPK$^{+/+}$ MEFs at time zero without lysosomal inhibitors. However, there is LC3-II found at time zero for AMPK$^{-/-}$ MEFs without lysosomal inhibitors. Additionally, an incremental increase in LC3-II formation was observed for AMPK$^{+/+}$ and AMPK$^{-/-}$ MEFs over the 20 hour time course and this increase was significantly greater in AMPK$^{-/-}$ than AMPK$^{+/+}$ MEFs (Figure 4A). Upon addition of 3-MA, the increase in LC3-II was largely blunted and showed no increase at the later time points (12-20 hours) (Figure 4B).

3-Methyladenine inhibition of autophagy in both AMPK$^{+/+}$ and AMPK$^{-/-}$ MEFs leads to increased apoptosis. In order to determine whether the autophagic pathway contributes to survival in AMPK$^{-/-}$ and AMPK$^{+/+}$ MEFs, we utilized 3-methyladenine (3-MA), a known autophagy inhibitor, to observe its effects on MEFs under both serum-rich and serum free conditions. Indeed 7mM 3-MA treatment for 20 hours caused increased apoptosis in AMPK$^{+/+}$ cells under nutrient deprivation conditions as indicated by activation of caspase-3 and PARP (Figure 5A). This was confirmed with the Annexin-V FITC/PI Apoptosis assay (Figure 5B). Interestingly, the increase of apoptotic cell death in AMPK$^{+/+}$ cells under nutrient deprivation with 3-MA was similar to serum deprived AMPK$^{-/-}$ MEFs without 3-MA. Such observation would suggest there is a functional autophagic pathway in AMPK$^{-/-}$ cells supported by increased apoptosis when AMPK$^{-/-}$ MEFs are treated with 3-MA compared to non-treated (Figure 5). Both cell types utilize some autophagy under basal nutrient rich conditions as both AMPK$^{+/+}$ and AMPK$^{-/-}$ cells showed some increase in apoptosis when treated with 3-MA. Additionally, the AMPK$^{-/-}$ cells exhibited much more apoptosis, suggestive of their increased reliance on autophagy under nutrient-rich conditions (Figure 5B). However, we do note that although 3-MA is widely used to inhibit autophagy, targets of 3-MA at 7mM may also include additional pathways such as the Akt survival pathway. Therefore, we do not rule out the possibility of off-target pathways that may play a part in the observed cell death. Therefore we decided to verify the 3-MA observation by knocking down an essential autophagy gene, ATG7, *via* a shRNA expressing plasmid under low glucose no serum conditions for 20 hours. However, we did not observe increased cell death as with the 3-MA treatment (Figure 5C). Therefore, we may only suggest the

increased cell death observed in both AMPK$^{-/-}$ and wildtype 3-MA treated cells could in part be due to autophagy inhibition but also other pathways. Although we cannot exclude that the remaining (~15%) of ATG7 could still have some function.

Reduced ATP levels in AMPK$^{-/-}$ cells. We next tested whether ATP levels were similar in AMPK$^{+/+}$ and AMPK$^{-/-}$ MEFs. We hypothesized that ATP levels might be similar or even elevated in AMPK$^{-/-}$ cells due to the increased basal level of autophagy. However, despite increased basal levels of autophagy, we observed ~50% decrease in ATP levels in AMPK$^{-/-}$ MEFs cultured under low glucose conditions compared to wildtype MEFs and AMPK null MEFs cultured in high glucose. Additionally, there was an ~30% reduction in ATP levels in AMPK null MEFs compared to wildtype MEFs under low glucose-serum containing conditions (Figure 6A). Furthermore, high glucose media conditions revealed no significant difference in ATP levels between AMPK$^{+/+}$ and AMPK$^{-/-}$ MEFs. This indicates the energy sensor, AMPK, becomes essential once the cells are starved of glucose and serum. Although, MEFs contain hexokinase, which has a lower Km for glucose than glucokinase, our observations may be due to glucose consumption during the time course of the experiment.

Further, to explore whether the cell death that occurs under serum starvation may simply be the result of not enough ATP, we added methyl pyruvate, a cell-permeable form of pyruvate to cells. Pyruvate can be decarboxylated to acetyl-coenzyme A, which can enter the Tricarboxylic Acid Cycle (TCA) to produce energy. Interestingly, although we did not observe a statistically significant increase in the ATP level with methylpyruvate treatment, cell viability was maintained for AMPK$^{-/-}$ cells during serum deprivation treated with methyl pyruvate (Figure 6B). Further, lysate harvested from

cells after 20 hours of methyl pyruvate treatment under serum rich and serum deprived conditions revealed a decrease in LC3-II for AMPK$^{-/-}$ cells under both conditions (Figure 6C). Additionally, we observed that AMPK$^{-/-}$ cells cultured in high glucose do not show increased basal levels of autophagy again suggesting the energy sensor, AMPK, becomes vital during times of reduced ATP levels.

Increased p53 phosphorylation and PTEN induction in AMPK$^{-/-}$ cells. p53 is a well characterized tumor suppressor gene activated by numerous cellular stressors and genotoxic insults. p53 regulates various cellular functions including cell growth, DNA repair, senescence, apoptosis and even autophagy.[40-42] Although some investigators demonstrate that p53 activates autophagy [40, 41, 43-45] other studies suggest that p53 inhibits autophagy.[40-42, 46] In most cases by ultimately affecting mTOR possibly through PTEN or the TSC1/2 complex.

p53 phosphorylation, specifically at serine 15 (ser15) is induced during glucose starvation suggesting a role of p53 coupling cellular energy and metabolism with cell growth.[43] Additionally, another study found that ultraviolet (UV) and hydrogen peroxide stress activated AMPK and p53 phosphorylation at ser15 to mediate stress induced apoptosis[47]. Therefore we wanted to determine whether p53 phosophorylation is induced in our samples during serum fed or deprived conditions, and if phosphorylation status correlates with protein levels of upstream regulators of mTOR including PTEN and tuberin (TSC2). Western blot analysis did reveal upregulation of p53 phosphorylation at Ser15 in AMPK$^{-/-}$ cells compared to wildtype when cultured under low glucose conditions (Figure 7A). Furthermore, PTEN and tuberin levels were increased in AMPK$^{-/-}$ cells when cultured in low glucose medium. Our results suggest that AMPK$^{-/-}$ cell

susceptibility to apoptosis correlates with increased Ser15 p53 phosphorylation in response to lower ATP levels. Moreover, we observed no significant difference between AMPK$^{-/-}$ and wildtype cells for the above-mentioned markers when cultured in high glucose conditions (Figure 7B).

Discussion

Autophagy can be induced during pathogenic invasion, starvation conditions, or stress as a means of maintaining homeostasis and viability. Altered regulation of autophagy - either as disease causing or disease treating - has received interest in many therapeutic areas including cancer, heart disease, neurodegeneration, lysosmal storage disease, and infectious disease.[8, 13, 18, 19, 48-51] More recent studies have tried to understand the link between autophagy and apoptosis. Conceptually, AMPK and autophagy can both be activated under times of stress in order to restore energetic homeostasis. In addition, like autophagy, activation of AMPK has been suggested to promote cell death under very specific conditions, for instance in cancer cells.

Examination of molecular signaling events could help elucidate these context dependent differential outcomes. However, interpretation of experiments can be confounded by the use of pharmacological inhibitors or RNA interference based approaches, both of which can have off-target effects. It is important to note that much of the research to date investigating AMPK's role in autophagy has used pharmacological agents such as AICAR to activate AMPK. However, there is evidence suggesting that AICAR's effects can be independent of AMPK even though many studies suggest AMPK (through AICAR) induces autophagy. [32, 39, 52] A past study[35] demonstrated that AICAR is

able to maintain inhibitory effects on glucose phosphorylation in both wildtype and AMPKα double knockout primary hepatocytes, suggesting an AMPK-independent but AICAR-dependent effect. Clearly it is of vital importance to investigate AMPK's role in any phenotype in the absence of activating or inhibiting pharmacological agents that may have AMPK-independent effects. Previous studies[53, 54] did use AMPK α1/α2 double knockouts to investigate AMPK activity on autophagy during hypoxic conditions and in response to metformin treatment. Although one group suggests AMPK regulates hypoxia-induced autophagy via mTOR inhibition, this study did not detect LC3-II in either WT or KO cells but based autophagy on the amount of LC3-I because their antibody did not recognize LC3-II (nor did they use lysosomal inhibitors). The other study showed impaired relocalization of LC3 in $AMPK^{-/-}$ MEFs upon metformin treatment indicating that metformin-induced activation of autophagy is AMPK dependent. Our current study did not use pharmacological agents to activate or inhibit AMPK to examine its roles in autophagy and apoptosis and does not conclude that AMPK could not normally regulate autophagy, only that it is not required for its induction in response to serum starvation under low glucose.

AMPK, autophagy and p53 have conceptual similarities. A large body of literature suggests that AMPK, autophagy, and p53 can have either pro-survival or cell death promoting activity. Many conflicting observations could simply reflect differences in contexts, for example different cell types or different means of initiating stress that may lead to distinct outcomes. In any case, as more and more genetically engineered mice become available *in vivo* studies may more clearly define the roles of these molecules/processes without relying on pharmacological agents.

p53 - like AMPK - can also be activated under numerous stress conditions including glucose deprivation, heavy metal exposure and UV radiation all of which induce phosphorylation at serine 15.[43, 55, 56] Interestingly, both serine 15 and serine 46 of p53 can be phosphorylated under stress, however, only serine 15 is conserved between mice and humans. Additionally, p53 (Ser15) activation leads to increased levels of PTEN and TSC2 resulting in mTOR inhibition[43]. p53 has long been known to induce cell cycle arrest, cellular senescence or apoptosis in response to genotoxic agents in order to allow cells to recover from damage or promote apoptosis if the cellular damage is irreversible, respectively. Only recent investigation of AMPK function has explored its roles in cell cycle and cancer, while conversely more recent studies of p53 have explored its potential roles in metabolism.[57]

Do deficits in AMPK lead to increased autophagy generally? Our study, using genetically deficient AMPK cells, demonstrates that autophagy has a pro-survival role in $AMPK^{-/-}$ MEFs under low glucose, however, additional energetic stress burden on these cells leads to apoptosis perhaps *via* a p53 based mechanism (Figure 8). This study demonstrates, that AMPKα double knockout mouse embryonic fibroblasts have a high level of basal autophagy when cultured in low glucose. The data does not mean that AMPK does not have a role in modulating or even inducing autophagy under other medium conditions or contexts. Although our experiments in the presence of lysosomal inhibitors reveal some functional autolysosomal degradation in knockout cells, we cannot exclude the possibility that low ATP levels themselves could impair autophagic function by for instance impairing the lysosomal proton pump.

Two other possible explanations for the acceleration of autophagy in AMPK$^{-/-}$ MEFs under low glucose conditions exist. It has been proposed that mTOR itself is an ATP sensor and its activity falls as the ATP concentration decreases, thus removing an autophagic brake[58]; second, amino acids are essential for mTOR activation and in the absence of AMPK under low glucose concentrations, amino acids would be increasingly oxidized to provide energy and thus decrease activation of mTOR.

Researchers have shown various other molecules can have dual roles in regulating autophagy. For instance, p53 can either induce or inhibit autophagy.[40, 41] Therefore, it is plausible, depending on the cellular context, that AMPK could help induce autophagy during energetic stress, but serum starvation-low glucose induced autophagy does not require AMPK activation, at least in MEFs. Interestingly, both autophagy and AMPK are conserved from yeast to man but may have evolved slightly different regulatory pathways due to distinct outcomes needed for different cell types in multicellular organisms. Further *in vivo* studies utilizing AMPKα knockouts, especially in hepatocytes, would further elucidate AMPK's role in autophagy.

Materials and Methods

Plasmids, reagents, and antibodies. The following plasmids, reagents, and antibodies were used in the study: pLC3-venus was a kind gift from Dr. Fan Wang (Duke University). 3-methyladenine (3-MA) (Sigma: M9281), Rapamycin (LC Laboratories: R-5000), E64d, pepstatin A (Calbiochem: 330005, 516481), methylpyruvate (Sigma: 371173), anti-LC3 (MBL International: PM036), anti-phosphoAMPK (Cell Signal: 2535), anti-PARP(cleaved)(Cell Signal: 9544), anti-

Caspase 3 (Cell Signal: 9662), anti-Caspase 3 (cleaved)(Cell Signal: 9661), anti-PTEN(Cell Signal: 9556), anti-p53(Ser15)(Cell Signal: 9284), anti-p53(Cell Signal: 2524), anti-ACC(Ser79)(Cell Signal: 3661), anti-AMPKα(rabbit)(Cell Signal: 2603), anti- AMPKα(mouse) (Abcam: ab51025), anti-Tuberin (Santa Cruz: sc-893), anti-ATG7 and anti-α tubulin (Sigma: A2856 and T5168). Apoptosis Detection Kit was purchased from R & D Systems (TA4638). ATP Assay Kit was purchased from Sigma-Aldrich (FLASC).

Cell culture. All experiments were carried out in low glucose DMEM unless otherwise mentioned. AMPKα1/2 double knock-out mouse embryonic fibroblasts (MEFs) and wildtype controls (C57/B6) were grown in Dulbecco's Modified Eagle's Medium (DMEM) (Sigma: 6429 and 6046) containing 10% fetal bovine serum (Atlanta Biologicals: S11150) and 1X Pen/Strep antibiotics (Sigma: P4333) under 10% CO_2 and 37°C. For all experiments, cells were plated in either DMEM-H (4.5g/L) or DMEM-L (1g/L) and allowed to grow for 24-48 hours to reach 60-80% confluency before treatment for indicated times with E64d (10μg), pepstatin A (10μg), rapamycin (200nM), 3-MA (7mM), and methyl pyruvate (10mM).

Venus-LC3 transfections. Mouse embryonic fibroblasts were plated on 6-well cell culture plates containing coverslides. Cells were transfected with 4μg of venus-LC3 plasmid using Lipofectamine 2000 (Invitrogen: 11668-027). 36 hours post-transfection cells were treated with rapamycin under serum rich states or with E64d and pepstatin A under serum deprived conditions. 20 hours later the cells were washed with phosphate-buffered saline and fixed with 4% paraformaldehyde. Slides were mounted with Vectashield mounting media containing 4', 6'-diamidino-2-phenylindole (DAPI) (Vector

Laboratories: H-1200). Signals were observed by confocal microscopy with a Zeiss confocal microscope (LSM 510).

ATG7 shRNA knockdown. A retroviral vector encoding a short hairpin RNA (shRNA) construct against mouse ATG7 (TRCN0000092163) was obtained from UNC shRNA/Open Biosystems Core. A non-silencing (nonsense) short hairpin RNA vector was also obtained (RHS4080). MEF cultures were plated at a density to yield 60-70% confluency by the next day. Cultures were transfected using Lipofectamine 2000, according to the instructions provided by the manufacturer with ATG7 or non-silencing shRNA. 48 hours post transfection cells underwent 20 hours of serum deprivation. ATG7 protein level was analyzed by western blot analyses 3 days following transfection.

Western blotting. Cells were scraped via cell lifter (Corning) and harvested in culture medium and centrifuged at 1000 RPM for 5 min. Pellet was washed 2X in cold DPBS and lysed in ice-cold lysis buffer containing 25mM Tris(pH7.5), 2mM $MgCl_2$, 600mM NaCl, 2mM EDTA, 0.5% NP-40, and 1X protease and phosphatase cocktail inhibitors(Sigma). Aliquots of the Proteins were separated on 4–12% NuPAGE BisTris (Invitrogen: NP0321 and NP0322) or 12% NuPAGE BisTris (Invitrogen: NP0341 and NP0342) and then transfer to a polyvinylidene difluoride (PVDF) membrane (Amersham Biosciences: IPFL00010). After transfer, the membrane was washed 3X in TBS, blocked for 1 hour at room temperature in 5% Bovine Serum Albumin (BSA) in TBS, followed by 4°C overnight incubation with appropriate primary antibody in 5% BSA-TBS. Western blot analysis was performed at 1:1000 dilution of all primary antibodies with the following exception anti-α tubulin(1:16,000). Next day, the membrane was washed 3X in TBS-tween, incubated at room temperature for 1 hour with IRDye infrared secondary

antibody (LI-COR Biosciences: 926-32221 and 926-32210) at 1:2000 dilution in 5% BSA-TBS, followed by 2X TBS-T and 1X TBS washes. Scanning, analyzing, and quantification of blots were performed via the Odyssey Infrared Imaging System. Three or more independent experiments were performed for all immunoblotting data. Quantification data is represented by bar graphs with error bars that indicate the standard error of the mean.

Apoptosis assay: Annexin V-FITC detection. Apoptosis Detection kit from R&D Systems was used to detect apoptosis according to the manufacturer's instructions. Briefly, after collecting and washing twice with cold PBS, the treated and/or untreated cells were resuspended in a total of 100ul of Annexin V incubation solution containing 10x Binding Buffer (10ul) (10 mM HEPES/NaOH, pH 7.4, 150 mM NaCl, 1mM $MgCl_2$, 1.8mM $CaCl_2$), FITC-Annexin-V (1µl) and Propidium iodide (10ul), and ddH_2O (79ul). The samples were then incubated for 15 min in the dark at room temperature and then subjected to analytic flow cytometry using the Dako CyAn instrument through the flow cytometry core facility at UNC-Chapel Hill. The X-axis dot plot reflects the Annexin V-FITC fluorescence and the Y-axis the propidium iodide fluorescence.

ATP assay. Intracellular ATP levels were determined using the ATP bioluminescence assay kit from Sigma-Aldrich based on the manufacturer's instructions. Briefly, cells were harvested and 100µl of ATP Assay mix working solution was added to each well and allowed to incubate at room temperature for 3 minutes. During incubation 100µl of 1X ATP releasing reagent, 50µl of ultra pure H_2O, and 50µl of either cell lysate or standard were added and mixed. After the 3 minutes of incubation period 100µl of the

ATP Releasing agent mixture was added to wells containing ATP Assay mix solution, mixed and immediately measured via Fluoroskan Ascent (Thermo Scientific).

Statistical Analysis. For all quantified experiments, data is present as mean ± SEM. Analysis of Variance (ANOVA) was used to determine the statistical significance with significance set at 0.05. For Western blot quantification, independent experiments (cell preparation, cell harvest, and SDS-PAGE/transfer) were done three times (unless otherwise noted). Indirect immunofluorescent detection of secondary antibody (LI-COR) was scanned and standardized to an internal standard (tubulin) to calculate and quantify arbitrary units using the Odyssey Infrared Imaging System with a representative Western blot shown in each figure. For the Annexin V-FITC apoptosis detection, experiments were done independently four times and plotted in bar graph format, in addition a representative dot plot analysis of flow cytometry results is shown in the respective figure.

References

1. Yu L, Lenardo MJ, Baehrecke EH. Autophagy and caspases: a new cell death program. Cell Cycle 2004; 3:1124-6.
2. Levine B, Sinha S, Kroemer G. Bcl-2 family members: dual regulators of apoptosis and autophagy. Autophagy 2008; 4:600-6.
3. Lockshin RA, Zakeri Z. Apoptosis, autophagy, and more. Int J Biochem Cell Biol 2004; 36:2405-19.
4. Maiuri MC, Zalckvar E, Kimchi A, Kroemer G. Self-eating and self-killing: crosstalk between autophagy and apoptosis. Nat Rev Mol Cell Biol 2007; 8:741-52.
5. Tsujimoto Y, Shimizu S. Another way to die: autophagic programmed cell death. Cell Death Differ 2005; 12 Suppl 2:1528-34.
6. Vicencio JM, Galluzzi L, Tajeddine N, Ortiz C, Criollo A, Tasdemir E, et al. Senescence, apoptosis or autophagy? When a damaged cell must decide its path--a mini-review. Gerontology 2008; 54:92-9.
7. Wang Y, Singh R, Massey AC, Kane SS, Kaushik S, Grant T, et al. Loss of macroautophagy promotes or prevents fibroblast apoptosis depending on the death stimulus. J Biol Chem 2008; 283:4766-77.
8. Cuervo AM. Autophagy and aging: keeping that old broom working. Trends Genet 2008; 24:604-12.

9. Klionsky DJ, Abeliovich H, Agostinis P, Agrawal DK, Aliev G, Askew DS, et al. Guidelines for the use and interpretation of assays for monitoring autophagy in higher eukaryotes. Autophagy 2008; 4:151-75.
10. Mizushima N, Yoshimori T. How to interpret LC3 immunoblotting. Autophagy 2007; 3:542-5.
11. Tanida I, Minematsu-Ikeguchi N, Ueno T, Kominami E. Lysosomal turnover, but not a cellular level, of endogenous LC3 is a marker for autophagy. Autophagy 2005; 1:84-91.
12. Tanida I, Ueno T, Kominami E. LC3 conjugation system in mammalian autophagy. Int J Biochem Cell Biol 2004; 36:2503-18.
13. Todde V, Veenhuis M, van der Klei IJ. Autophagy: Principles and significance in health and disease. Biochim Biophys Acta 2009; 1792:3-13.
14. Cuervo AM, Dice JF. A receptor for the selective uptake and degradation of proteins by lysosomes. Science 1996; 273:501-3.
15. Majeski AE, Dice JF. Mechanisms of chaperone-mediated autophagy. Int J Biochem Cell Biol 2004; 36:2435-44.
16. Massey AC, Kaushik S, Sovak G, Kiffin R, Cuervo AM. Consequences of the selective blockage of chaperone-mediated autophagy. Proc Natl Acad Sci U S A 2006; 103:5805-10.
17. Galluzzi L, Morselli E, Vicencio JM, Kepp O, Joza N, Tajeddine N, et al. Life, death and burial: multifaceted impact of autophagy. Biochem Soc Trans 2008; 36:786-90.
18. Gozuacik D, Kimchi A. Autophagy as a cell death and tumor suppressor mechanism. Oncogene 2004; 23:2891-906.
19. Nishida K, Yamaguchi O, Otsu K. Crosstalk between autophagy and apoptosis in heart disease. Circ Res 2008; 103:343-51.
20. Amodeo GA, Rudolph MJ, Tong L. Crystal structure of the heterotrimer core of Saccharomyces cerevisiae AMPK homologue SNF1. Nature 2007; 449:492-5.
21. Carling D, Aguan K, Woods A, Verhoeven AJ, Beri RK, Brennan CH, et al. Mammalian AMP-activated protein kinase is homologous to yeast and plant protein kinases involved in the regulation of carbon metabolism. J Biol Chem 1994; 269:11442-8.
22. Gao G, Fernandez CS, Stapleton D, Auster AS, Widmer J, Dyck JR, et al. Non-catalytic beta- and gamma-subunit isoforms of the 5'-AMP-activated protein kinase. J Biol Chem 1996; 271:8675-81.
23. Hardie DG, Carling D, Carlson M. The AMP-activated/SNF1 protein kinase subfamily: metabolic sensors of the eukaryotic cell? Annu Rev Biochem 1998; 67:821-55.
24. Williams T, Brenman JE. LKB1 and AMPK in cell polarity and division. Trends Cell Biol 2008; 18:193-8.
25. Crute BE, Seefeld K, Gamble J, Kemp BE, Witters LA. Functional domains of the alpha1 catalytic subunit of the AMP-activated protein kinase. J Biol Chem 1998; 273:35347-54.
26. Stapleton D, Gao G, Michell BJ, Widmer J, Mitchelhill K, Teh T, et al. Mammalian 5'-AMP-activated protein kinase non-catalytic subunits are homologs of

proteins that interact with yeast Snf1 protein kinase. J Biol Chem 1994; 269:29343-6.
27. Woods A, Munday MR, Scott J, Yang X, Carlson M, Carling D. Yeast SNF1 is functionally related to mammalian AMP-activated protein kinase and regulates acetyl-CoA carboxylase in vivo. J Biol Chem 1994; 269:19509-15.
28. Hedbacker K, Carlson M. SNF1/AMPK pathways in yeast. Front Biosci 2008; 13:2408-20.
29. Wang Z, Wilson WA, Fujino MA, Roach PJ. Antagonistic controls of autophagy and glycogen accumulation by Snf1p, the yeast homolog of AMP-activated protein kinase, and the cyclin-dependent kinase Pho85p. Mol Cell Biol 2001; 21:5742-52.
30. Liang J, Shao SH, Xu ZX, Hennessy B, Ding Z, Larrea M, et al. The energy sensing LKB1-AMPK pathway regulates p27(kip1) phosphorylation mediating the decision to enter autophagy or apoptosis. Nat Cell Biol 2007; 9:218-24.
31. Matsui Y, Takagi H, Qu X, Abdellatif M, Sakoda H, Asano T, et al. Distinct roles of autophagy in the heart during ischemia and reperfusion: roles of AMP-activated protein kinase and Beclin 1 in mediating autophagy. Circ Res 2007; 100:914-22.
32. Meley D, Bauvy C, Houben-Weerts JH, Dubbelhuis PF, Helmond MT, Codogno P, et al. AMP-activated protein kinase and the regulation of autophagic proteolysis. J Biol Chem 2006; 281:34870-9.
33. Samari HR, Moller MT, Holden L, Asmyhr T, Seglen PO. Stimulation of hepatocytic AMP-activated protein kinase by okadaic acid and other autophagy-suppressive toxins. Biochem J 2005; 386:237-44.
34. Samari HR, Seglen PO. Inhibition of hepatocytic autophagy by adenosine, aminoimidazole-4-carboxamide riboside, and N6-mercaptopurine riboside. Evidence for involvement of amp-activated protein kinase. J Biol Chem 1998; 273:23758-63.
35. Guigas B, Bertrand L, Taleux N, Foretz M, Wiernsperger N, Vertommen D, et al. 5-Aminoimidazole-4-carboxamide-1-beta-D-ribofuranoside and metformin inhibit hepatic glucose phosphorylation by an AMP-activated protein kinase-independent effect on glucokinase translocation. Diabetes 2006; 55:865-74.
36. Jacobs RL, Lingrell S, Dyck JR, Vance DE. Inhibition of hepatic phosphatidylcholine synthesis by 5-aminoimidazole-4-carboxamide-1-beta-4-ribofuranoside is independent of AMP-activated protein kinase activation. J Biol Chem 2007; 282:4516-23.
37. Kuo CL, Ho FM, Chang MY, Prakash E, Lin WW. Inhibition of lipopolysaccharide-induced inducible nitric oxide synthase and cyclooxygenase-2 gene expression by 5-aminoimidazole-4-carboxamide riboside is independent of AMP-activated protein kinase. J Cell Biochem 2008; 103:931-40.
38. Nofziger C, Kalsi K, West TA, Baines D, Blazer-Yost BL. Vasopressin regulates the phosphorylation state of AMP-activated protein kinase (AMPK) in MDCK-C7 cells. Cell Physiol Biochem 2008; 22:487-96.
39. Viana R, Aguado C, Esteban I, Moreno D, Viollet B, Knecht E, et al. Role of AMP-activated protein kinase in autophagy and proteasome function. Biochem Biophys Res Commun 2008; 369:964-8.

40. Tasdemir E, Chiara Maiuri M, Morselli E, Criollo A, D'Amelio M, Djavaheri-Mergny M, et al. A dual role of p53 in the control of autophagy. Autophagy 2008; 4:810-4.
41. Zong WX, Moll U. p53 in autophagy control. Cell Cycle 2008; 7:2947.
42. Tasdemir E, Maiuri MC, Galluzzi L, Vitale I, Djavaheri-Mergny M, D'Amelio M, et al. Regulation of autophagy by cytoplasmic p53. Nat Cell Biol 2008; 10:676-87.
43. Feng Z, Zhang H, Levine AJ, Jin S. The coordinate regulation of the p53 and mTOR pathways in cells. Proc Natl Acad Sci U S A 2005; 102:8204-9.
44. Jin S. p53, Autophagy and tumor suppression. Autophagy 2005; 1:171-3.
45. Maiuri MC, Tasdemir E, Criollo A, Morselli E, Vicencio JM, Carnuccio R, et al. Control of autophagy by oncogenes and tumor suppressor genes. Cell Death Differ 2009; 16:87-93.
46. Morselli E, Tasdemir E, Maiuri MC, Galluzzi L, Kepp O, Criollo A, et al. Mutant p53 protein localized in the cytoplasm inhibits autophagy. Cell Cycle 2008; 7:3056-61.
47. Cao C, Lu S, Kivlin R, Wallin B, Card E, Bagdasarian A, et al. AMP-activated protein kinase contributes to UV- and H2O2-induced apoptosis in human skin keratinocytes. J Biol Chem 2008; 283:28897-908.
48. Easton JB, Houghton PJ. mTOR and cancer therapy. Oncogene 2006; 25:6436-46.
49. Martinez-Vicente M, Talloczy Z, Kaushik S, Massey AC, Mazzulli J, Mosharov EV, et al. Dopamine-modified alpha-synuclein blocks chaperone-mediated autophagy. J Clin Invest 2008; 118:777-88.
50. Takagi H, Matsui Y, Hirotani S, Sakoda H, Asano T, Sadoshima J. AMPK mediates autophagy during myocardial ischemia in vivo. Autophagy 2007; 3:405-7.
51. Winslow AR, Rubinsztein DC. Autophagy in neurodegeneration and development. Biochim Biophys Acta 2008; 1782:723-9.
52. Meijer AJ, Codogno P. AMP-activated protein kinase and autophagy. Autophagy 2007; 3:238-40.
53. Papandreou I, Lim AL, Laderoute K, Denko NC. Hypoxia signals autophagy in tumor cells via AMPK activity, independent of HIF-1, BNIP3, and BNIP3L. Cell Death Differ 2008; 15:1572-81.
54. Buzzai M, Jones RG, Amaravadi RK, Lum JJ, DeBerardinis RJ, Zhao F, et al. Systemic treatment with the antidiabetic drug metformin selectively impairs p53-deficient tumor cell growth. Cancer Res 2007; 67:6745-52.
55. Matsuoka M, Igisu H. Cadmium induces phosphorylation of p53 at serine 15 in MCF-7 cells. Biochem Biophys Res Commun 2001; 282:1120-5.
56. Melnikova VO, Santamaria AB, Bolshakov SV, Ananthaswamy HN. Mutant p53 is constitutively phosphorylated at Serine 15 in UV-induced mouse skin tumors: involvement of ERK1/2 MAP kinase. Oncogene 2003; 22:5958-66.
57. Ma W, Sung HJ, Park JY, Matoba S, Hwang PM. A pivotal role for p53: balancing aerobic respiration and glycolysis. J Bioenerg Biomembr 2007; 39:243-6.
58. Dennis PB, Jaeschke A, Saitoh M, Fowler B, Kozma SC, Thomas G. Mammalian TOR: a homeostatic ATP sensor. Science 2001; 294:1102-5.

Figure Legends

Figure 1. AMPK$^{-/-}$ MEFs demonstrate increased apoptosis under low glucose-serum deprivation. Cells were cultured in low (A) and high glucose (B) for analysis of AMPK$^{-/-}$ and AMPK$^{+/+}$ MEFs with Annexin V-FITC (X-axis) and Propidium Iodide (PI) (Y-axis) labeling. Predominantly viable cells with a small amount of cell death are shown (A, a-c and B, a-d). However, AMPK$^{-/-}$ low glucose-serum deprived MEFs demonstrate increased cell death mostly annexin and/or annexin PI positive, indicating apoptotic death (A, d). Quantification of low (A) and high (B) glucose for Annexin V-PI experiments (C). Western blot analysis indicates that under nutrient–rich (low glucose-serum containing) conditions AMPK$^{+/+}$ and AMPK$^{-/-}$ MEFs do not have activation of caspases or cleavage of the downstream target PARP (poly ADP ribose polymerase) (D). However, 20 hours serum deprivation leads to increased caspase activation and cleaved PARP in AMPK$^{-/-}$ MEFs. (E) Levels of total AMPK and phosphorylated ACC. For all figures AMPK$^{-/-}$ indicates the absence of AMPKα1 and AMPKα2. 40μg of whole cell lysate was run on a 4-12% Bis-Tris SDS PAGE gel. Annexin+ cells /viable cells and PI+ cells/viable cells quantification is denoted by the bar graph with indicated standard deviation from 4 independent experiments.

Figure 2. Accumulated venus-LC3 puncta in AMPK$^{-/-}$ MEFs under low glucose-serum rich conditions suggestive of elevated autophagy. AMPK$^{+/+}$ and AMPK$^{-/-}$ MEFs cultured in low (A-J) or high glucose (K-O) were transiently transfected with venus-LC3 plasmid. 24 hours post-transfection cells were either treated with rapamycin (**B, C, G, H, L, M**) or cultured in serum-free media plus or minus protease inhibitors (**D, E, I, J, N, O**) for 20

hours. Cells were fixed in 4% paraformaldehyde for 15 minutes and mounted onto slides for imaging. Representative percentages of transfected cells: A>90%; B, C>65%; D, E>50%; F-H >75%; K>90%; L-O>70%. 400X magnification was used for all images (some with digital magnification as well); scale bar represent 10μm. Images without scale bars used the same magnification as 2A. A-O is representative of 3 independent experiments.

Figure 3. Increased Autophagy as indicated by endogenous LC3-II formation in $AMPK^{-/-}$ MEFs. (A) Endogenous LC3 was analyzed by immunoblotting in $AMPK^{+/+}$ and $AMPK^{-/-}$ MEFs cultured in nutrient rich complete DMEM medium with 10% FBS or treated with E64d (10μg/ml) and pepstatin A (10μg/ml) inhibitors. A total of 45μg of whole cell lysate was used for immunoblotting on 12% Bis-Tris NuPage Gel. (B) $AMPK^{-/-}$ and $AMPK^{+/+}$ MEFs were cultured in serum-free medium for 20 hours treated with either protease inhibitors/vehicle and 35μg of whole cell lysate was evaluated on a 4-12% Bis-Tris SDS PAGE gel. Bar graphs represent quantification of LC3-II/Tubulin ratio for 4 independent experiments. Error bars represent standard deviation.

Figure 4. Time Course of autophagic flux as indicated by endogenous LC3-II formation in $AMPK^{-/-}$ MEFs. Whole cell lysate (35μg) from cells cultured in serum-free medium for 0, 2, 6, 12, and 20 hours and treated with either E64d and pepstatin A lysosomal inhibitors (A) was used for immunoblotting to detect endogenous levels of LC3. Additionally, cells cultured in serum-free medium for 0, 2, 6, 12, and 20 hours were also treated with lysosomal inhibitors plus 3-MA (B) and lysate (35μg) was used to

determine the level of autophagic flux via LC3-II formation. The ratio of LC3-II to tubulin is represented by the bar graphs, which also includes error bars to depict the standard deviation.

Figure 5. The autophagy inhibitor 3-Methyladenine (3-MA) increases apoptosis in serum deprived MEFs. MEFs were cultured in serum-free medium for 20 hours and treated with 3-MA or vehicle and 40µg of whole cell lysate run on a 4-12% Bis-Tris NuPAGE gel and immunoblotted (A). Analysis of $AMPK^{-/-}$ and $AMPK^{+/+}$ MEFs via Annexin V-FITC and Propidium Iodide labeling demonstrates $AMPK^{+/+}$ serum deprived MEFs treated with 3-MA results in an increased amount of apoptosis which is comparable to $AMPK^{-/-}$ serum deprived MEFs without 3-MA (B). 3-MA treated $AMPK^{-/-}$ MEFs without serum leads to even greater apoptosis. Additionally, $AMPK^{+/+}$ MEFs were transfected with an ATG7 or non-silencing (NS) shRNA. 48 hours post transfection cells underwent 20 hours of serum deprivation and 40ug of whole cell lysate was used to analyze ATG7 protein levels by western blot analyses (C) (NS= non-silencing shRNA). Annexin+ cells /viable cells and PI+ cells/viable cells quantification denoted by the bar graph with indicated standard deviation representing 4 independent experiments.

Figure 6. Decreased ATP levels in $AMPK^{-/-}$ MEFs under low glucose-serum containing conditions. Cells were plated in either DMEM-H (4.5g/L) or DMEM-L (1g/L) containing serum and allowed to grow for 36 hours to reach 80% confluency. After 36 hours cells were maintained in serum-free DMEM or serum-rich DMEM for an additional 20 hours. (A) Under low glucose serum rich conditions $AMPK^{-/-}$ MEFs have

substantially lower ATP levels. **H** indicates the use of high glucose medium while **L** indicates low glucose medium. Results represent 2 independent experiments performed in triplicate. Samples were normalized to wild type levels in serum-high glucose conditions. Error bars indicate standard deviation. (B) Whole cell lysate (35μg) from $AMPK^{-/-}$ and $AMPK^{+/+}$ cells treated with methyl pyruvate rescues caspase activation during serum starvation and (C) decreases LC3-II ratios compared to vehicle, analyzed by Western blot on 4-12% (B) and 12% (C) Bis-Tris NuPage gels. LC3/tubulin quantification is denoted by the bar graph with indicated standard deviation of 3 independent experiments.

Figure 7. Increased p53 phosphorylation at Serine 15 (Ser15) and increased PTEN in $AMPK^{-/-}$ cells. Western blot analysis reveals increased phosphorylated p53 and PTEN levels for $AMPK^{-/-}$ cells under either serum starved or serum containing media when cultured in low glucose (A) but not during high glucose cultured conditions (B). Bar graphs represent quantification of indicated protein relative to tubulin, including the standard error of the mean for 3 independent experiments.

Figure 8. The absence of AMPK activity results in cell death under nutrient stress. Normal ($AMPK^{+/+}$) cells induce autophagy (green double circles) under nutrient stress to generate ATP and promote cell survival. Cells lacking AMPK activity have elevated basal autophagy and cannot generate sufficient energy following nutrient stress. In the presence of phosphorylated p53 (purple circle; “P”) the cells then undergo apoptosis.

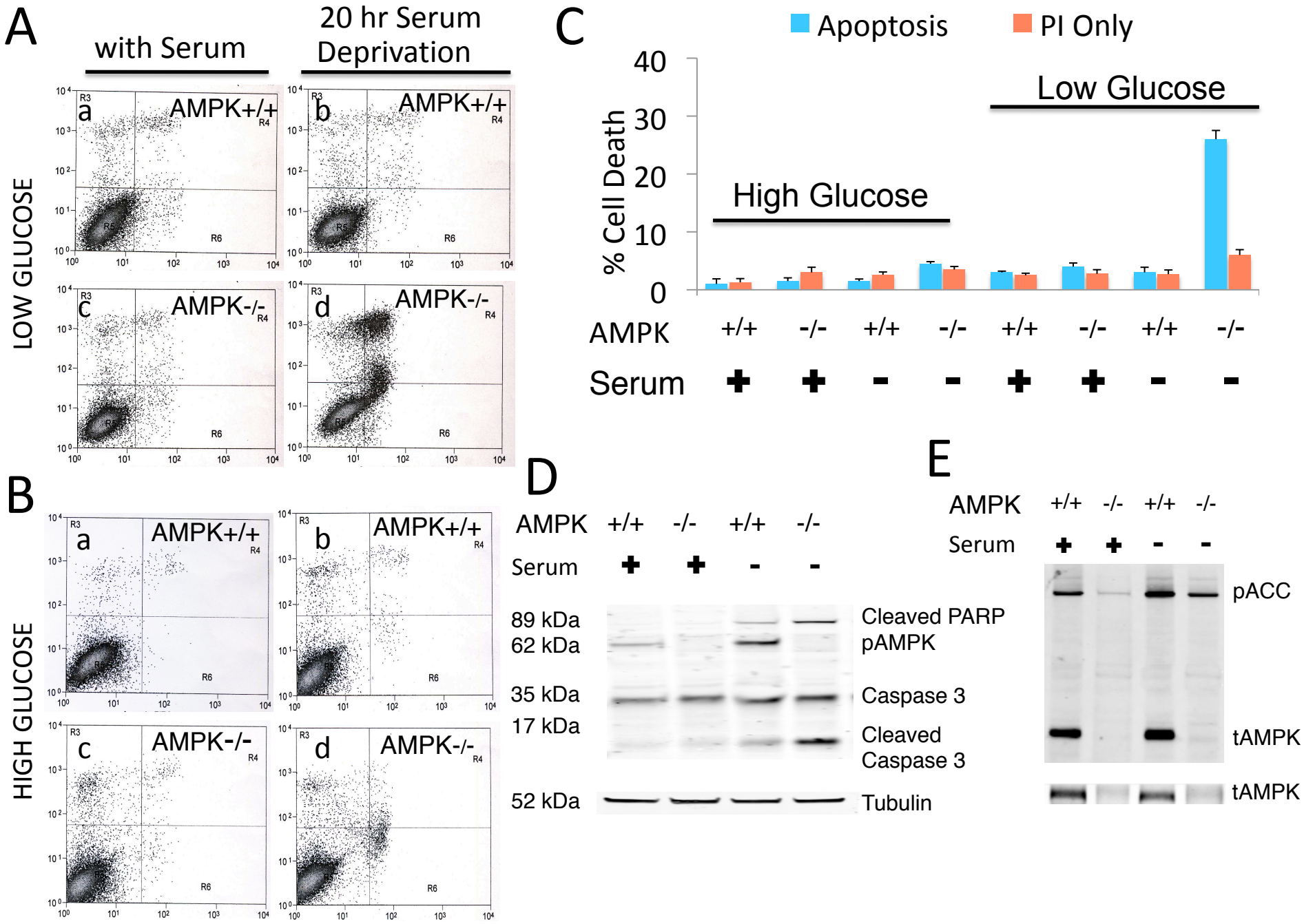
A
with Serum
20 hr Serum Deprivation
LOW GLUCOSE
a AMPK+/+
b AMPK+/+
c AMPK-/-
d AMPK-/-
B
HIGH GLUCOSE
a AMPK+/+
b AMPK+/+
c AMPK-/-
d AMPK-/-
C
Apoptosis
PI Only
% Cell Death
40
30
20
10
0
Low Glucose
High Glucose
AMPK +/+ -/- +/+ -/- +/+ -/- +/+ -/-
Serum + + - - + + - -
D
AMPK +/+ -/- +/+ -/-
Serum + + - -
89 kDa
62 kDa
35 kDa
17 kDa
52 kDa
Cleaved PARP
pAMPK
Caspase 3
Cleaved Caspase 3
Tubulin
E
AMPK +/+ -/- +/+ -/-
Serum + + - -
pACC
tAMPK
tAMPK

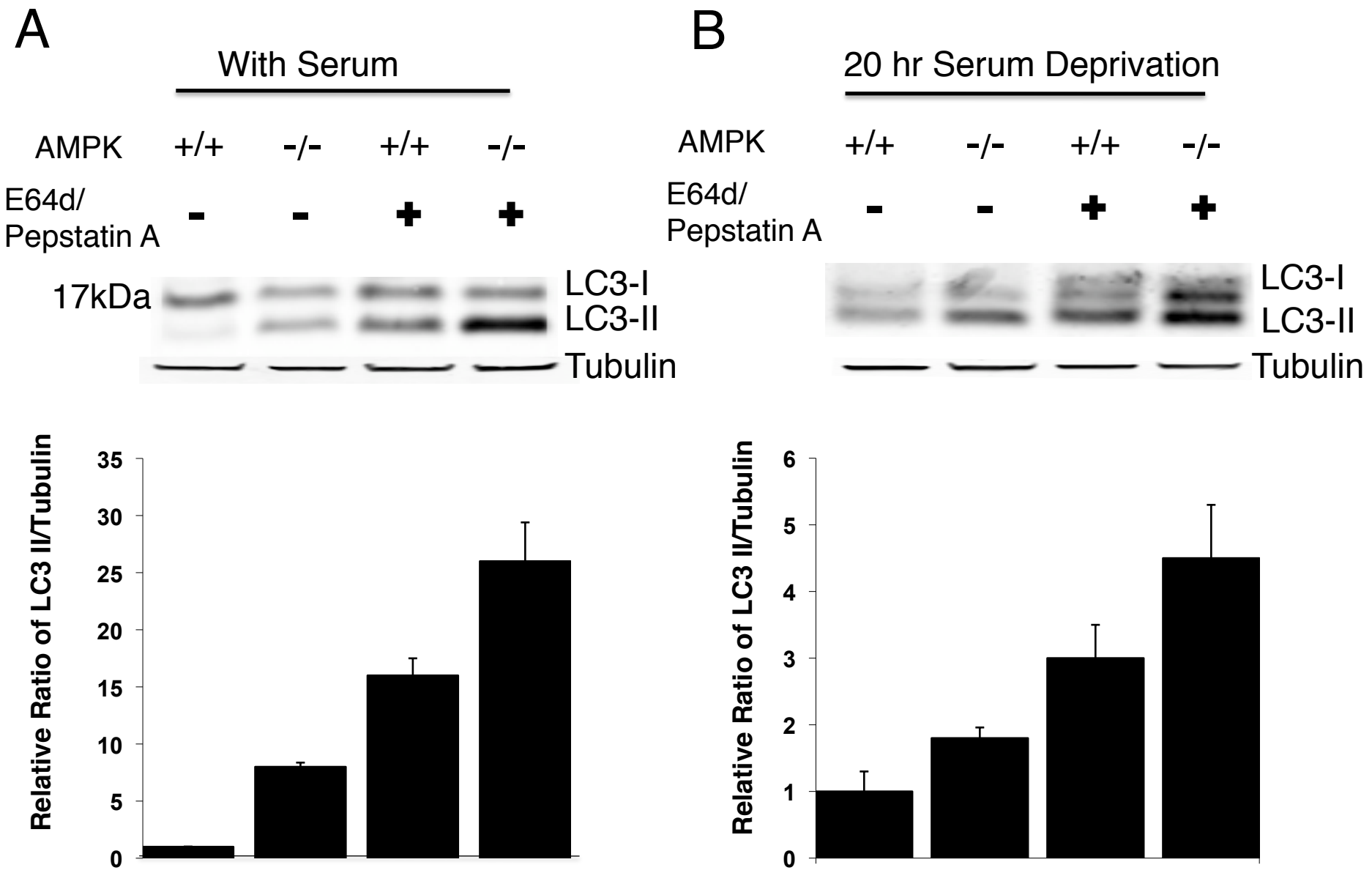
A
With Serum
AMPK
+/+
-/-
+/+
-/-
E64d/
Pepstatin A
-
-
+
+
17kDa
LC3-I
LC3-II
Tubulin
B
20 hr Serum Deprivation
AMPK
+/+
-/-
+/+
-/-
E64d/
Pepstatin A
-
-
+
+
LC3-I
LC3-II
Tubulin
Relative Ratio of LC3 II/Tubulin
35
30
25
20
15
10
5
0
Relative Ratio of LC3 II/Tubulin
6
5
4
3
2
1
0

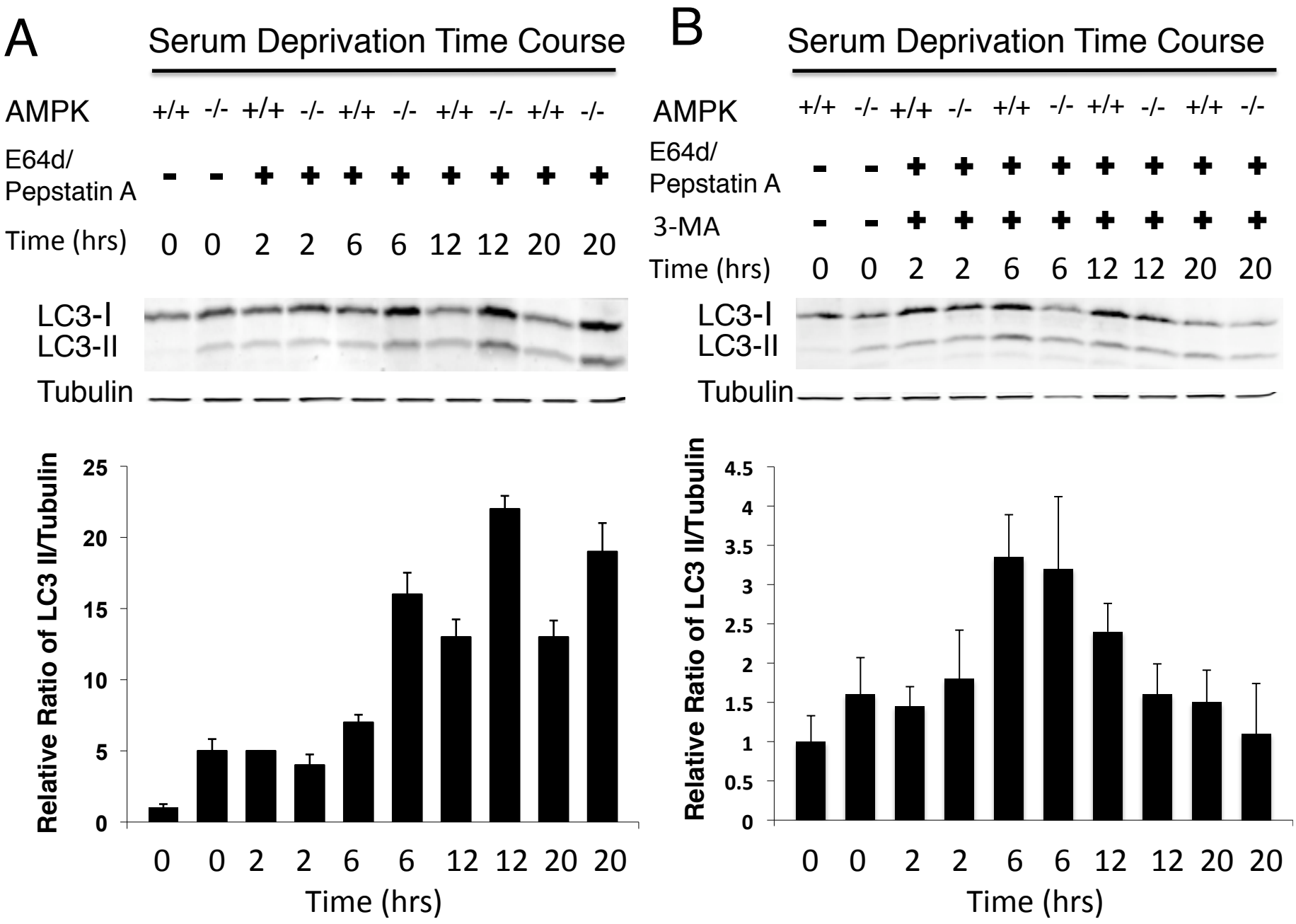
A
Serum Deprivation Time Course
AMPK
+/+ -/- +/+ -/- +/+ -/- +/+ -/- +/+ -/-
E64d/
Pepstatin A
- - + + + + + + + +
Time (hrs)
0 0 2 2 6 6 12 12 20 20
LC3-I
LC3-II
Tubulin
Relative Ratio of LC3 II/Tubulin
25
20
15
10
5
0
0 0 2 2 6 6 12 12 20 20
Time (hrs)
B
Serum Deprivation Time Course
AMPK
+/+ -/- +/+ -/- +/+ -/- +/+ -/- +/+ -/-
E64d/
Pepstatin A
- - + + + + + + + +
3-MA
- - + + + + + + + +
Time (hrs)
0 0 2 2 6 6 12 12 20 20
LC3-I
LC3-II
Tubulin
Relative Ratio of LC3 II/Tubulin
4.5
4
3.5
3
2.5
2
1.5
1
0.5
0
0 0 2 2 6 6 12 12 20 20
Time (hrs)

A

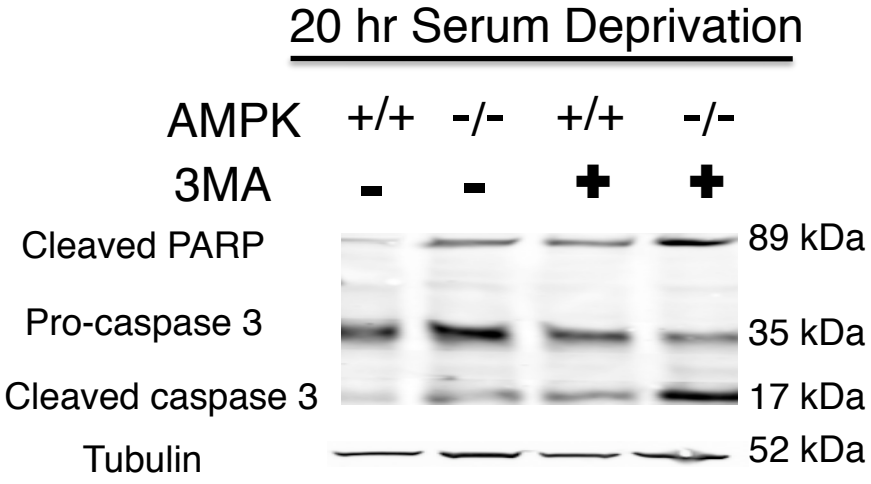
20 hr Serum Deprivation
AMPK +/+ -/- +/+ -/-
3MA - - + +
Cleaved PARP
Pro-caspase 3
Cleaved caspase 3
Tubulin
89 kDa
35 kDa
17 kDa
52 kDa

B

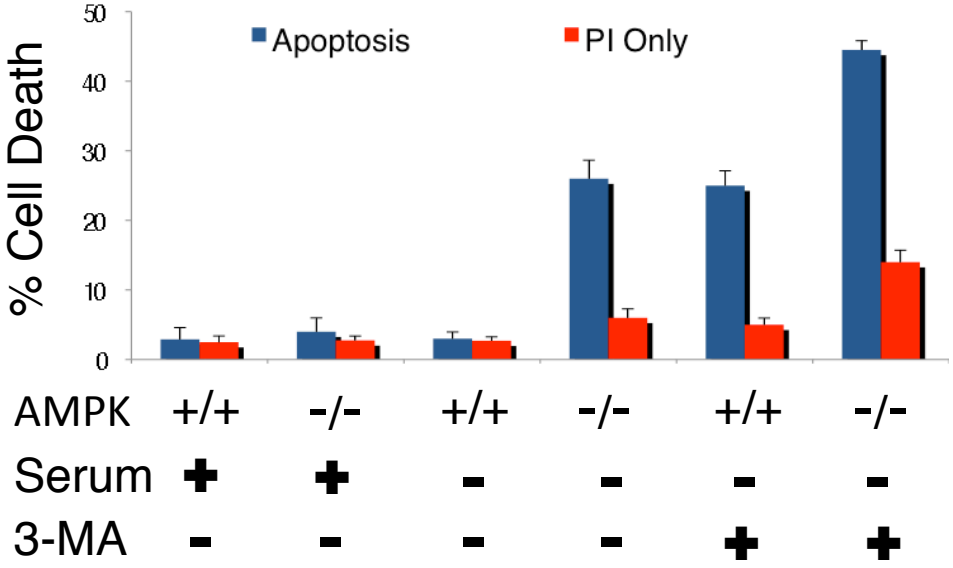
% Cell Death
50
40
30
20
10
0
Apoptosis
PI Only
AMPK +/+ -/- +/+ -/- +/+ -/-
Serum + + - - - -
3-MA - - - - + +

C

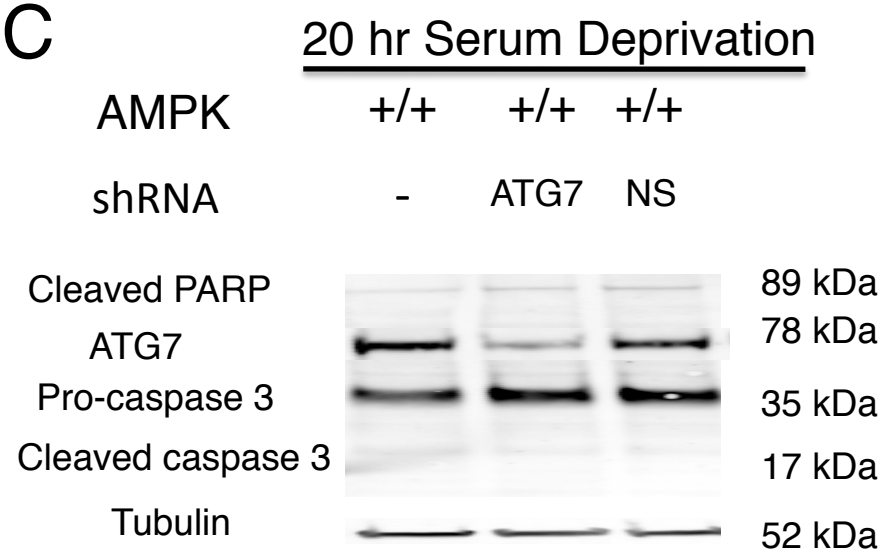
20 hr Serum Deprivation
AMPK +/+ +/+ +/+
shRNA - ATG7 NS
Cleaved PARP
ATG7
Pro-caspase 3
Cleaved caspase 3
Tubulin
89 kDa
78 kDa
35 kDa
17 kDa
52 kDa

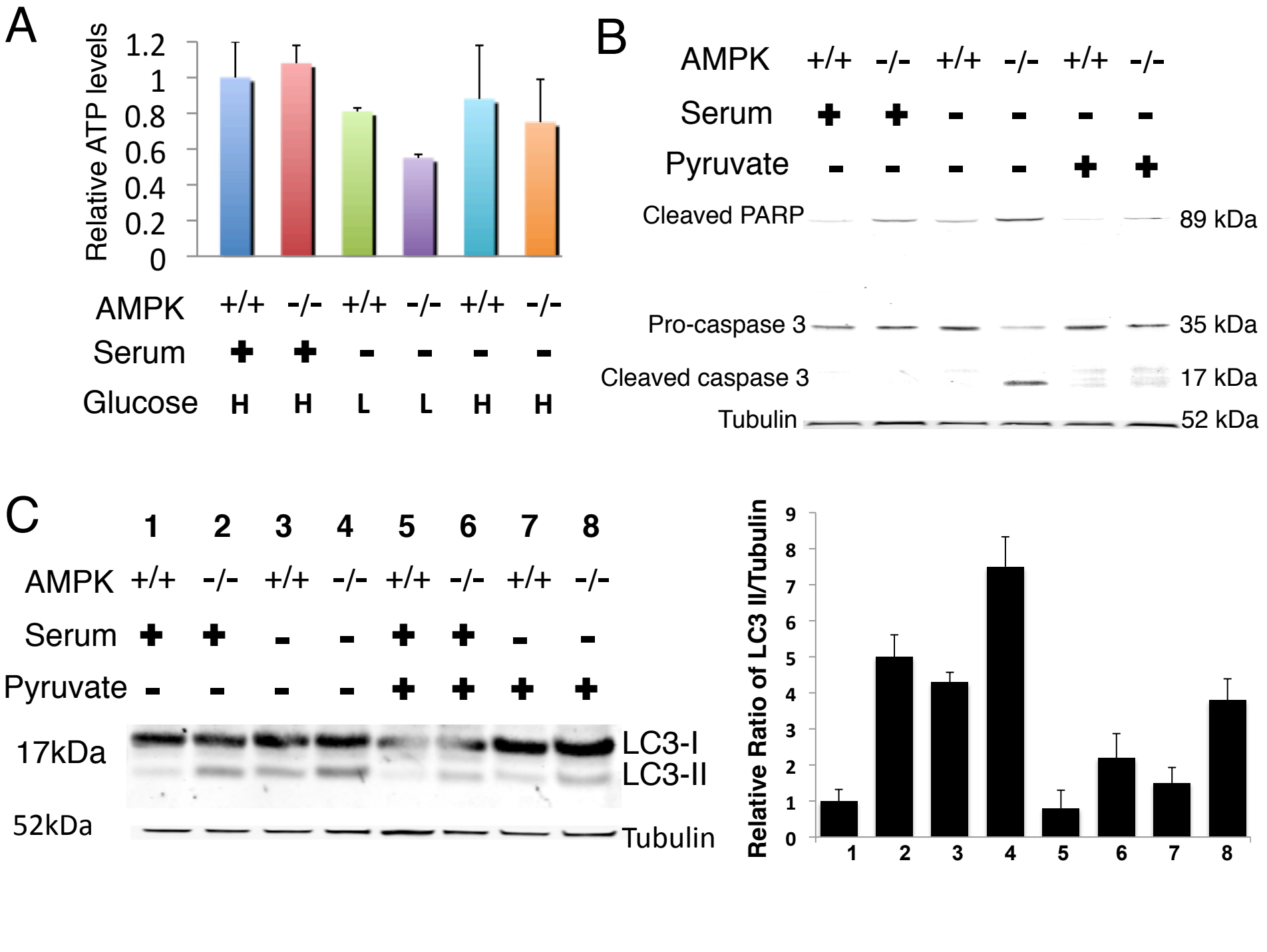
A
Relative ATP levels
1.2
1
0.8
0.6
0.4
0.2
0
AMPK +/+ -/- +/+ -/- +/+ -/-
Serum + + - - - -
Glucose H H L L H H
B
AMPK +/+ -/- +/+ -/- +/+ -/-
Serum + + - - - -
Pyruvate - - - - + +
Cleaved PARP
89 kDa
Pro-caspase 3
35 kDa
Cleaved caspase 3
17 kDa
Tubulin
52 kDa
C
1 2 3 4 5 6 7 8
AMPK +/+ -/- +/+ -/- +/+ -/- +/+ -/-
Serum + + - - + + - -
Pyruvate - - - - + + + +
17kDa
LC3-I
LC3-II
52kDa
Tubulin
Relative Ratio of LC3 II/Tubulin
9
8
7
6
5
4
3
2
1
0
1 2 3 4 5 6 7 8

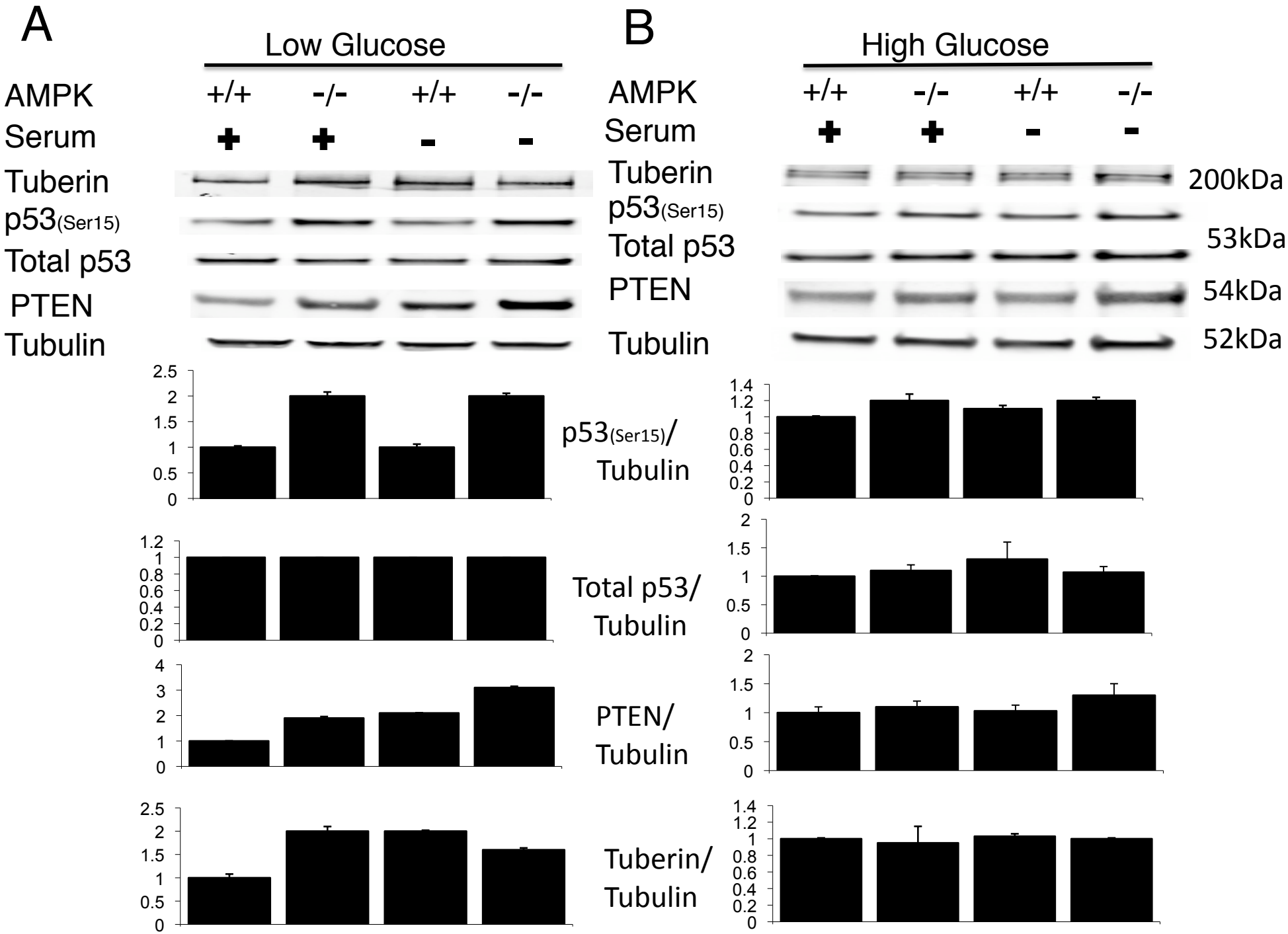
A
Low Glucose
AMPK
+/+
-/-
+/+
-/-
Serum
+
+
-
-
Tuberin
p53(Ser15)
Total p53
PTEN
Tubulin
B
High Glucose
AMPK
+/+
-/-
+/+
-/-
Serum
+
+
-
-
Tuberin
p53(Ser15)
Total p53
PTEN
Tubulin
200kDa
53kDa
54kDa
52kDa
p53(Ser15)/ Tubulin
Total p53/ Tubulin
PTEN/ Tubulin
Tuberin/ Tubulin

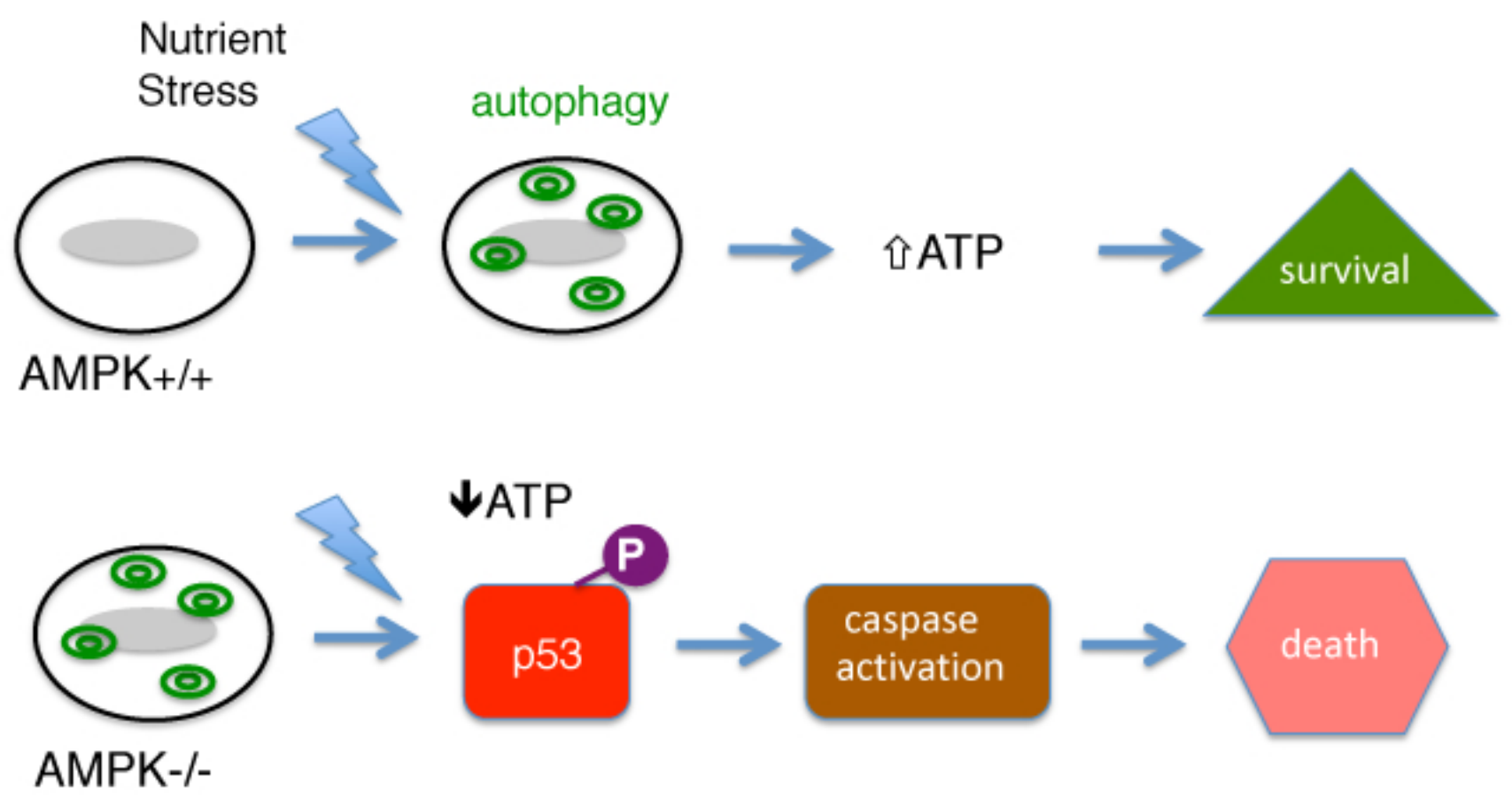
Nutrient
Stress
autophagy
⇧ATP
survival
AMPK+/+
⇩ATP
P
p53
caspase
activation
death
AMPK-/-